JBC Papers in Press. Published on January 31, 2012 as Manuscript M111.319764
The latest version is at http://www.jbc.org/cgi/doi/10.1074/jbc.M111.319764

Increasing Serum Half-life and Extending Cholesterol Lowering *in vivo* by Engineering an Antibody with pH-sensitive Binding to PCSK9

Javier Chaparro-Riggers*[1], Hong Liang*[1], Rachel M. DeVay[1], Lanfang Bai[1], Janette E. Sutton[1], Wei Chen[1], Tao Geng[1], Kevin Lindquist[1], Meritxell Galindo Casas[1], Leila M. Boustany[1], Colleen L. Brown[1], Jeffrey Chabot[1], Bruce Gomes[2], Pamela Garzone[1], Andrea Rossi[1], Pavel Strop[1], Dave Shelton[1], Jaume Pons[1,3], and Arvind Rajpal[1,3]

[1]Rinat-Pfizer Inc., 230 East Grand Avenue, South San Francisco, CA 94080, USA
[2]Novartis Institutes for BioMedical Research, Inc, 45 Sidney Street, Cambridge, MA 02139, USA

*: equal contribution
[3] To whom correspondence should be addressed at: Rinat-Pfizer Inc., 230 East Grand Avenue, South San Francisco, CA 94080, USA: Email: Jaume.Pons@pfizer.com & Arvind.Rajpal@pfizer.com

Running title: *Increasing PK and PD in vivo by a pH-sensitive antibody*

Background: An antagonistic anti-PCSK9 antibody exhibit target-mediated clearance resulting in a dose-dependent PK.
Results: Engineering of an antibody with pH-sensitive binding to PCSK9 decreases target-mediated clearance resulting in increased PK and efficacy *in vivo*.
Conclusions: pH-sensitive anti-PCSK9 antibodies are excellent candidates for therapeutic development.
Significance: pH-sensitive antibodies may enable less frequent or lower dosing of antibodies hampered by target-mediated clearance and high antigen load.

SUMMARY:
Target-mediated clearance and high antigen load can hamper the efficacy and dosage of many antibodies. We show for the first time that the mouse, cynomolgus and human cross-reactive, antagonistic anti-Proprotein Convertase Substilisin Kexin type 9 (PCSK9) antibodies J10 and the affinity matured and humanized J16 exhibit target-mediated clearance, resulting in dose-dependent pharmacokinetic (PK) profiles. These antibodies prevent the degradation of Low Density Lipoprotein Receptor (LDLR) thus lowering serum levels of LDL-cholesterol (LDL-C) and potently reducing serum cholesterol in mice and selectively reduce LDL-C in cynomolgus monkeys. In order to increase the PK and efficacy of this promising therapeutic for hypercholesterolemia, we engineered pH-sensitive binding to mouse, cynomolgus and human PCSK9 into J16, resulting in J17. This antibody shows prolonged half-life and increased duration of cholesterol lowering in two species *in vivo* by binding to endogenous PCSK9, in mice and cynomolgus monkeys, respectively. The proposed mechanism of this pH sensitive antibody is that it binds with high affinity to PCSK9 in the plasma at pH 7.4, while the antibody-antigen complex dissociates at the endosomal pH of 5.5-6.0 in order to escape from target-mediated degradation. Additionally, this enables the antibody to bind to another PCSK9 and therefore increasing the antigen-binding cycles. Furthermore, we show that this effect is dependent on the neonatal Fc receptor (FcRn), which rescues the dissociated antibody in the endosome from degradation. Engineered pH-sensitive antibodies may enable less frequent or lower dosing of antibodies hampered by target-mediated clearance and high antigen load.

INTRODUCTION
Therapeutic antibodies represent the fastest-growing class of therapeutics in the pharmaceutical marketplace (1). Improving efficacy of antibodies through engineering have mainly concentrated on the Fc-portion for increased half-life (2,3) and effector function (4) and on the variable region for improved affinity. Still several antibodies have to be dosed at high frequency or high dose in order to obtain therapeutic efficacy, often based on the high synthesis rates and/or antigen-mediated degradation of the antibody, e.g. C5, IgE, IL6R.

Antibodies with pH-dependent binding to the antigen could improve the efficacy in case that the antibody binds tightly to the antigen in the plasma (pH 7.4) and the antibody-antigen complex would dissociate in the acidic endosome. This would allow the antibody to undergo further binding cycles and/or mitigate from target-mediated degradation by dissociation of the antigen-antibody complex in the acidic endosome. We applied this method to an anti PCSK9 antibody.

PCSK9 has been implicated as a major regulator of plasma LDL-C (5) and has emerged as a promising target for prevention and treatment of coronary heart disease (CHD). Human genetic studies identified gain-of-function mutations, which were associated with elevated serum levels of LDL-C and premature incidences of CHD, whereas loss-of-function mutations were associated with low LDL-C and reduced risk of CHD(6-9). In humans, the complete loss of PCSK9 results in low serum LDL-C of <20 mg/dL, in otherwise healthy subjects (10,11).

PCSK9 belongs to the subtilisin family of serine proteases and is composed of an N-terminal prodomain, a subtilisin-like catalytic domain and a C-terminal cysteine/histidine-rich domain (CHRD). Highly expressed in the liver and intestine, PCSK9 is secreted after the autocatalytic cleavage of the prodomain, which remains non-covalently associated with the catalytic domain (12,13). The catalytic domain of PCSK9 binds to the epidermal growth factor-like repeat A (EGF-A) domain of LDLR with higher affinity in the endosomal pH of approximately 5.5-6.0 than in plasma at 7.4 (14). Although the C-terminal domain does not bind to LDLR it has been proposed to be involved in the internalization of the LDLR-PCSK9 complex (15-17). Both functionalities of PCSK9 are required for targeting the LDLR-PCSK9 complex for lysosomal degradation and lowering LDL-C, which is in agreement with mutations in both domains linked to loss- and gain-of-function (5).

Various therapeutic approaches for inhibiting PCSK9 have been reported, including gene silencing by siRNA or anti-sense oligonucleotides and disruption of the PCSK9-LDLR interaction by antibodies (18). Two monoclonal antibodies with LDL-C lowering activity in mice and non-human primates (19,20) were reported to have unexplained short half-lives of approximately 2.5 (19) and 3.2 days (20) in non-human primates at 3 mg/kg. We have reported antibodies J10 and J16 that reduced serum cholesterol in mice and monkey (21). Here we present that these antibodies exhibit a dose-dependent half-life, and that this increased *in vivo* clearance was PCSK9-dependent. To enhance the pharmacokinetic (PK) and pharmacodynamic (PD) properties of the antibody, we engineered pH-sensitive binding to PCSK9 (antibody J17) by introducing histidines into CDR residues, as has been described in other systems (22-24). We demonstrate that we are able to prolong half-life and increase duration of cholesterol lowering through inhibition of endogenous PCSK9 in two species *in vivo*. Finally, we were able to show that this process is dependent on the neonatal Fc receptor (FcRn).

EXPERIMENTAL PROCEDURES

Proteins and antibodies- Recombinant human, mouse and cynomolgus PCSK9 proteins, antibody J10 and J16 were produced and made as previously described (21). J17 was obtained by combining three histidine mutations, which were identified by a histidine-scanning mutagenesis in all CDR positions of J16.

J10, J16 and J17 concentration measurement in mouse serum-Mouse sera were collected at indicated time points. NUNC maxisorp 96-well plates (Invitrogen) were coated with recombinant mouse PCSK9 at 5 µg/ml in PBS and incubated overnight at 4°C. Plates were washed then blocked for 1 hour at room temperature in 3% BSA in PBS at 300 µl/well. J10, J16 or J17 antibody standards were prepared in dilution buffer (0.5% BSA, 0.05% Tween-20 in PBS), with the starting concentration of 0.5µg/ml. Serum samples were diluted at 1:500 to 1:20,000 in dilution buffer. Samples and standards were incubated in the blocked plate for 1 hour at room temperature. Plates were washed, 100 µl of anti-mouse IgG (H+L) HRP (Jackson ImmunoResearch, cat# 715-035-150) (1:5,000 dilution in PBS, 0.5% BSA) was added to each well and plates were incubated at room temperature for 1 hour. Plates were washed and developed using SUREBLUE TMB 1-C SUBSTRATE solution (VWR, Cat #95059-284) following manufacture's instruction, and read on a Molecular Devices plate-reader at 450 nm. Data was analyzed using SoftMaxPro4.8, Microsoft Excel and Graphpad PRISM.

J16 and J17 concentration measurement in monkey serum and plasma-Monkey serum or K_2EDTA plasma was collected at indicated time points. Protocols are similar to that of the mouse serum measurement with the following changes: maxisorp plates were coated with 1ug/ml of anti-id antibodies, 26G8 and 20F5, for J16 and J17, respectively. 1 µg/ml of another murine anti-PCSK9 antibody was added to all samples and standards to minimize PCSK9 interference in the assay. Goat IgG anti-human Kappa HRP (MP Biomedicals) was used as secondary.

Mouse studies-All mouse studies were conducted in accordance with the Institutional Animal Care and Use Committee at Pfizer Inc. Male *C57BL/6* were purchased from Charles River labs; *FCRN* $^{-/-}$ mice and *PCSK9* $^{-/-}$ mice (12,25) were licensed and purchased from Jackson Labs. Mice were bred at the facility or acclimated to the facility for two weeks prior to the start of experiments. Animals were 6-10 weeks of age at the start of each experiment. Animals were housed conventionally under ambient conditions, with free access to water and standard rodent chow.

Monkey studies-The dose response for J16 in cynomolgus monkeys was previously reported (21). The J16 and J17 comparison study were done similarly, using a total of 8 male adult cynomolgus macaque (*Macaca fascicularis*). All animal maintenance and handling is in accordance with the Institutional Animal Care and Use Committee at association for assessment and accreditation of laboratory animal care international (AAALAC) accredited facility.

Lipid analysis of serum and plasma samples-Serum and plasma samples were analyzed for lipid measurements (total cholesterol, HDL-c, LDL-c, triglyceride) using Ace Alera clinical chemistry System (Alfa Wassermann). Results of lipid measurements were analyzed and graphed using GraphPad Prism software.

Binding Affinities-Affinity measurement of all variants to mouse, cynomolgus and human PCSK9 at pH 6.0 and 7.4 at 37°C were measured by Biacore T200 (GE Healthcare). The running buffers were 10 mM sodium phosphate, 150 mM NaCl, 0.05% Tween-20 (at pH 6 or 7.4). The sensor chip was an anti-human Fc surface (on a Biacore CM4 chip blocked with ethylenediamine). The capture levels of IgGs were 2 µg/mL. The top analyte concentration was 200 nM and the dilution factor was 3-fold.

Lysosomal colocalization of anti-PCSK9 antibodies in HepG2 cells-HepG2 cells were plated onto glass coverslips one day before and incubated in serum free media for at least 1 hour prior to the internalization assays. To assess antibody trafficking, we first mixed 5 µg/mL PCSK9 with 10 µg/mL of isotype control antibody, J10 or J17 and then added the mixture to HepG2 cells. After 6 hours, the cells were fixed with formaldehyde and permeabilized with 0.1% Triton X-100, 2 mg/ml BSA, PBS, 0.02% Tween-20. A standard immunofluorescence protocol was followed using anti-Lamp2 monoclonal antibody (ab25631, AbCam, Cambridge, MA) to stain lysosomes and Alexa-488 goat anti-mouse and Alexa-594 goat anti-human (Invitrogen, Carlsbad, CA) secondary antibodies. We followed a similar protocol to assess PCSK9 trafficking, except that PCSK9 was labeled with Alexa-488 using an Invitrogen protein labeling kit. Cells were imaged using a Leica TCS SPE Laser Scanning Confocal Microscope with a 63x 1.3 NA oil objective (Leica Microsystems, Manheim, Germany). Images were collected using a 0.5 µm step size and analyzed using Leica AF software. Antibody lysosomal colocalization was calculated as percent of total antibody puncta that were Lamp2 positive from at least 400 puncta from each of three experiments. PCSK9-488 lysosomal colocalization was calculated as percent of total PCSK9-488 puncta that were Lamp2 positive. Quantifications are shown as average with standard error; statistical significance was determined by student's t-test. Colocalization mask was created using Image J software and the colocalization plugin (NIH, Bethesda, MD).

RESULTS

Anti-PCSK9 antibody J16 shows a dose-dependent half-life in non-human primates. We have previously reported that a humanized and affinity matured anti-PCSK9 antibody with IgG2ΔA heavy chain and kappa light chain, J16, selectively and dose-dependently lowered LDL-C in cynomolgus monkeys. This antibody contains an IgG2 subclass variant with minimal FcγR binding (21). To further study the pharmacokinetics (PK) of J16, we measured total plasma antibody concentrations in monkeys treated with a single bolus intra

venous (i.v.) injection of 0.1, 1.0, 3.0, 10.0 and 100.0 mg/kg of J16. The estimated half-life during the β-elimination phase was 0.7 days at a single dose of 0.1 mg/kg, and increased to 1.9, 2.3, 3.5 and 5.3 days at 1.0, 3.0, 10.0 and 100.0 mg/kg, respectively (Fig. 1A, Table S1). Such dose-dependent antibody half-life is often observed with membrane associated antigens that exhibit antigen-mediated clearance (26).

PCSK9 mediates the enhanced clearance of circulating J10 in mice. To explore the possibility that PCSK9 can enhance the elimination of an anti-PCSK9 antibody, we studied the PK of J10, the precursor of J16 with a mouse IgG1, in wild type and *PCSK9* $^{-/-}$ mice (12). After a single bolus i.v. injection of 10 mg/kg of J10 and an isotype control, the half-life of the β-phase for J10 (3.5 days) was significantly shorter than that of the isotype control (7.4 days) in wild type mice, while the half-lives of the two antibodies were similar in *PCSK9*$^{-/-}$ mice (6.1 and 7.1 days, respectively) (Fig. 1B, 1C, Table S2).

Generation of an antibody with pH-sensitive binding to PCSK9. To avoid PCSK9-mediated shortening of antibody half-life, we aimed to engineer an antibody that has pH-sensitive binding to PCSK9. It shall have high affinity to PCSK9 at the neutral pH encountered in plasma to be effective in antigen binding, and low affinity to PCSK9 at the low pH of the endosome to enhance antibody dissociation from PCSK9, and thus potentially escape from PCSK9-mediated degradation. By histidine scanning of all the residues in the CDRs in J16, and through combination of effective mutations, we generated an antibody, J17, that exhibits a 3.8-, 2.6-, and 9.2-fold lower binding affinity at pH 6 compared to pH 7.4 for mouse, cynomolgus and human PCSK9, respectively (Table 1). Most of this pH dependent effect comes from the difference in the rate of dissociation of the complex (k_d) (Fig. S1). J17 contained histidine substitutions in CDR1 (S30H) and CDR2 (S50H) of the light chain and CDR2 (S52H) of the heavy chain. Modeling suggests that $His30_{J17}$ in CDR1 interacts with PCSK9 residue $Asp374_{PCSK9}$ which has been shown to be partially responsible for the pH dependence of the LDLR:PCSK9 interaction (14)(Fig. S2 and Supplemental text). While LDLR binds more tightly to PCSK9 at low pH, J17 shows opposite pH dependence and binds more tightly to PCSK9 at neutral pH. These data suggest that opposing pH dependencies can be achieved at the same interaction site, allowing the local environment to determine the direction of the pH effect.

J17 shows improved serum half-life and extends cholesterol lowering in mice and non-human primates. To facilitate *in vivo* studies, we grafted the J17 variable region onto mouse IgG1 for rodent studies and human IgG2ΔA frame work for non-human primate studies. The effect of J17-mIgG1 compared to J10 was studied in wild type mice at 1, 3 and 10 mg/kg doses. Antibody concentrations were monitored over 75 days. At 10 mg/kg, the β-elimination half-life for J17 was extended to 14.4 days, compared to 2.9 days for J10 (Fig. 2A, Table S3). At 1 and 3 mg/kg, the J10 antibody concentrations were below the assay's lower limit of detection before reaching the β-phase, while the half-lives for J17 were 13.7 and 12.9 days, respectively. These data suggest that the half-life of J17 is not only extended at all doses when compared to J10, its half-life is no longer dose-dependent during the timeframe of these experiments. Furthermore, the half-life of the β-phase for J17 was similar to that of the isotype control antibody at 10 mg/kg (9.4 days), suggesting that PCSK9-mediated degradation of J17 in circulation was significantly reduced (Fig. 2A, Table S3). To confirm the prolonged PK of J17-hIgG2ΔA in non-human primates, 1.5 mg/kg of J16 and J17 were injected i.v. into cynomolgus monkeys. J17 has an estimated half-life of 7.4 days compared to 0.9 days for J10 (Fig. 2B, Table S4). To ensure that the observed differences were not based on different affinities to FcRn, we confirmed similar affinities of J16 and J17 to cyno FcRn by surface plasmon resonance (SPR) (Fig. S3).

To explore whether the improved PK also results in improved duration of efficacy, total cholesterol levels were measured in mice treated with 1, 3, or 10 mg/kg of J10 or J17-mIgG1 over 75 days. The animals dosed with isotype control antibody display total cholesterol levels between 90 and 100 mg/dL throughout the study. The animals dosed with 1 mg/kg J10 show minimal change, 3 and 10 mg/kg doses of J10 lowers total cholesterol to 75 and 65 mg/dL at day 4, and recover to baseline levels at day 20 and 25, respectively (Fig. 2C). The 1, 3 and 10 mg/kg doses of J17 lowers total

cholesterol to 78, 75 and 65 mg/dL, and don't recover to baseline levels until day 75 (Fig. 2C). Compared to J10, J17 had equivalent magnitude of cholesterol lowering, with extended duration at all doses tested in mice. To confirm the enhanced cholesterol lowering effect of J17 in non-human primates, a single i.v. dose of 1.5 mg/kg J16 or J17 was injected in cynomolgus monkeys. Both J16 and J17 treatment lowers the LDL-C concentration by ~50% at peak efficacy. LDL-C in J16 treated animals starts to recover by day 4, and returns to baseline by day 10, while LDL-C in J17 treated animals starts to recovered only around day 10, and returns to baseline at day 30 (Fig. 2D).

J17 show reduced PCSK9-dependent lysosomal accumulation compared with J16. We next looked at cellular trafficking of J10 and J17 in a hepatic cell line in an effort to mechanistically understand whether the increased half-life of J17 is due to reduced lysosomal trafficking and degradation. To address this, we incubated HepG2 cells with PCSK9 in the presence of J10, J17, or an isotype control, and looked for lysosomal co-localization of the antibodies by laser scanning confocal microscopy (LCSM). We observed that both J10 and J17, but not the isotype control, are internalized when in the presence of PCSK9, and interestingly, that J10 is trafficked to lysosomes more effectively than J17 (Fig. 3A and 3B). Employing similar techniques, we determined that PCSK9 is trafficked to the lysosomes as efficiently in the presence of J10 and J17 as in the presence of the isotype control (Figure 3B). These results suggest that J17 is differentially trafficked away from lysosomes independently of PCSK9, thus rescuing J17 from PCSK9 mediated lysosomal degradation.

PCSK9 has minimal effect on J17 serum half-life. To further demonstrate that PCSK9 accelerates J10 clearance and that this effect is mitigated by J17, we studied the effect of the addition of exogenous recombinant human PCSK9 (huPCSK9) after dosing antibodies into *PCSK9* $^{-/-}$ mice. A dose of 10 mg/kg of J10, J17 and an isotype control was injected by intra-peritoneal (i.p.) route into *PCSK9* $^{-/-}$ mice. The three antibodies have similar serum concentrations throughout the first 14 days post injection. On day 15 of the experiment 3 mg/kg of recombinant huPCSK9 was administered i.v.. The J10 antibody concentration dropped to 24% of the previous day's value (day 14) one hour after the injection of huPCSK9, while the isotype control and J17 antibody concentration only dropped to 88% and 81%, respectively, during the same period (Fig. 4A). These results suggest that the introduced pH sensitivity of J17 protects the antibody from PCSK9-mediated degradation.

The prolonged serum half-life of J17 is FcRn-dependent. FcRn extends antibody half-life *in vivo* by protecting IgG from degradation, since the serum half-life of IgG are greatly reduced in *FCRN* $^{-/-}$ mice (25). To evaluate the role of FcRn in the PCSK9-mediated degradation of J10 and rescue of J17, we injected i.v. 10 mg/kg of J10, J17 and an isotype control into *FCRN* $^{-/-}$ mice. As expected the antibodies show faster clearance (Fig. 4B) compared to wild type mice (Fig. 1B, 2A). J10 and J17 both have half-lives of 0.7 days, shorter than that of the isotype control (1.1 days) (Fig. 4B). In comparison, the half-life for J17 (14.4 days) was comparable to that of the isotype control (9.4 days) and significantly longer than that of J10 (2.9 days) in wild type mice (Fig.2A, Table S3). Together these results suggest that the rescue of J17 from PCSK9-mediated degradation occurs through J17 binding to FcRn in acidic endosomal vesicles, and subsequent release to the circulation due to the increase in pH at the cell surface.

DISCUSSION

The two main mechanisms for active elimination of IgG are: a target-independent clearance pathway mediated by interaction between the Fc region on the antibody and the Fc receptors (FcRn and FcγR); and second, a target-mediated clearance pathway due to specific interaction between the Fab region of the antibody and its pharmacological target (27,28). Few soluble antigens undergo target-mediated elimination and often have dose-independent clearance rates for the soluble antibody-antigen complexes (29), which concomitantly lead to increased half-life of the antigen in complex with the antibody (30). An exception can be the elimination of the immune complexes through FcγR-mediated phagocytosis (26,30,31), when two or more antibodies bind simultaneously to one antigen. Target-mediated clearance result in dose-dependent elimination rates at different concentrations based on the saturable binding to the antigen. Antibodies targeting membrane-bound receptors often display

increased clearance by target-mediated degradation (29), where after binding to the receptor and receptor-mediated endocytosis, the receptor-antibody complex can be degraded.

Given the assumed 1 to 1 stoichiometry per binding site of J10 and J16 and the minimal FcγR binding of the IgG2ΔA subclass variant, we do not expect the formation of large complexes yielding a rapid clearance. However, despite this we clearly observe dose-dependent degradation of J16 (Fig. 1A). We confirmed antigen-mediated degradation by abrogation of increased elimination compared to isotype control antibody in *PCSK9*$^{-/-}$ animals (Fig. 1C) and hypothesize that the mechanism of PCSK9-mediated clearance of J10 may be similar to PCSK9-mediated lysosomal degradation of LDLR (5) given that the antibody shares an overlapping epitope on PCSK9 with LDLR (21). This is also suggested by confocal microscopy, showing that the J10-PCSK9 complex is co-localized in lysosomes compared to the isotype control (Fig. 3A).

In the past, methods for increasing the half-life of antibodies have mainly focused on increasing the affinity of Fc to FcRn (2,3) in order to decrease target-independent clearance. In the case of proteins other than antibodies, two groups have shown pH-dependent binding of engineered cytokines with increased dissociation in the endosome which correlate with increased recycling *in vitro* (24,32). Histidine has a pK_a of approximately 6 and is often found at the interfaces of proteins that interact with differential affinities in the plasma and endosome, such as FcRn (33) and human epidermal growth factor (32). Sakar et al. introduced histidines using a rational design on the granulocyte colony-stimulating factor (GCSF) region interacting with its cognate receptor (24). They maintained affinity at plasma's pH of 7.4, while the affinity was decreased at endosomal pH of 5.5 to 6.0 by putative protonation of these histidines. This led to increased recycling of the dissociated ligand and receptor to the cell surface, where they could bind to each other and signal again. Enhanced PK and PD *in vitro* were obtained by reducing degradation and allowing for repeated binding.

Recently, Igawa et al. generated a pH-dependent anti-human interleukin 6 receptor (IL6R) antibody by histidine scanning of the CDR's in tocolizumab (22). They measured the PK and PD in transgenic human IL6R animals by injecting human IL6 due to lack of rodent cross-reactivity in tocolizumab. These studies were unable to dissect the role of IL6 and IL6R synthesis *in vivo* and were further complicated by human IL6 binding to mouse and human IL6R. Despite these complications, the pH-sensitive antibody showed decreased clearance and increased inhibition of downstream serum amyloid A (SAA). They also demonstrated improved PK and PD for a pH-sensitive antibody containing enhanced FcRn binding mutations after injection of human IL6 daily and measuring the PD marker C-reactive protein (CRP) in monkeys. While the data were promising, the study combined mechanisms for reducing target-independent and target-mediated elimination simultaneously, confounding analysis of individual components.

In the present paper we engineered an anti-PCSK9 antibody to have pH sensitive antigen binding in an effort to enhance exposure, and reduced target mediated clearance. Our antibody is cross-reactive to mouse, cynomolgus and human PCSK9 allowing the measurement of PK and PD parameters in multiple *in vivo* models. As a PD and efficacy endpoint, we were able to measure the cholesterol lowering effect of the antibodies in mice and monkeys. We show that in wild-type mice J17 is able to abrogate target-mediated degradation, as seen by comparing its half-life to an isotype control (Fig. 2A). We were able to demonstrate this effect in *PCSK9*$^{-/-}$ mice after injecting human PCSK9 and showing that only the J10 serum concentration was reduced compared to J17 and the isotype control antibody (Fig. 3C). The total cholesterol levels of wild type mice injected with 10 mg/kg J10 and J17 were reduced to around 50% of the baseline level, with 2.8-fold increase in the duration of maximum efficacy by using J17. We also show improved PK and efficacy in monkeys at a 1.5 mg/kg dose, which results in a 2.5-fold improvement of the duration of the maximum effect and a 3-fold improvement of the recovery to baseline cholesterol levels using J17. These results suggest that the engineered pH-sensitivity leads to increased cycles of antigen binding, internalization, dissociation, antigen degradation, antibody recycling to the plasma, and binding fresh antigen. Our data suggests that J17 dissociates from PCSK9 in the endosome and minimizes target-mediated degradation, compared

to the parental antibody J10. Consistent with this, we saw decreased localization of J17 in the lysosome of HepG2 cells when co-incubated with PCSK9 (Fig. 3A and 3B). We hypothesized that this rescue can only occur if FcRn is also present in the same cell to recycle the antibody. In order to confirm this hypothesis, we measured the half-life of J10, J17 and an isotype control antibody in *FCRN*$^{-/-}$ mice (25), where we find that the difference in PK between J10 and J17 is minimized (Fig. 4B) suggesting the crucial role of FcRn in the rescue of J17 from PCSK9-mediated degradation. It is also interesting to note that while J17 showed comparable half-life to the isotype control in wild type animals (Fig. 2A), it shows faster elimination in *FCRN* $^{-/-}$ animals compared to the control antibody (Fig. 4B). This finding suggests that there may be other factors affecting J10 and J17 elimination in addition to PCSK9 and FcRn.

In the past, improving PK of antibodies was mainly obtained by engineering the Fc for increased affinity to FcRn, which may be less effective in addressing target-mediated degradation. The method presented here increases exposure by decreasing or eliminating target-mediated degradation, and has two potential beneficial effects for improving PD. First is to prevent the incomplete usage of antibodies bound to one antigen and subsequently degraded, and second is the recycling of free antibody resulting in increased antigen-binding cycles. In general, increasing efficacy of antibodies has conventionally been accomplished by improving affinity, especially for soluble antigens. In contrast, generating pH-sensitive antibodies is a balance of high affinity at pH 7.4 resulting in effective target occupancy, and fast dissociation kinetics (k_d) at pH 6.0, to facilitate antigen release in the endosome, resulting in enhanced PK and efficacy (22,24).

The applicability of this methodology has been shown for IL6R and PCSK9, but should be considered with care for new targets. High antigen concentration and rapid target-mediated degradation are situations where a pH-sensitive antibody may be beneficial however it is not clear how these two characteristics interplay in defining ideal targets.

REFERENCES

1. Nelson, A. L., Dhimolea, E., and Reichert, J. M. (2010) *Nat Rev Drug Discov* **9**, 767-774
2. Yeung, Y. A., Leabman, M. K., Marvin, J. S., Qiu, J., Adams, C. W., Lien, S., Starovasnik, M. A., and Lowman, H. B. (2009) *J Immunol* **182**, 7663-7671
3. Zalevsky, J., Chamberlain, A. K., Horton, H. M., Karki, S., Leung, I. W., Sproule, T. J., Lazar, G. A., Roopenian, D. C., and Desjarlais, J. R. (2010) *Nat Biotechnol* **28**, 157-159
4. Lazar, G. A., Dang, W., Karki, S., Vafa, O., Peng, J. S., Hyun, L., Chan, C., Chung, H. S., Eivazi, A., Yoder, S. C., Vielmetter, J., Carmichael, D. F., Hayes, R. J., and Dahiyat, B. I. (2006) *Proc Natl Acad Sci U S A* **103**, 4005-4010
5. Lambert, G., Charlton, F., Rye, K. A., and Piper, D. E. (2009) *Atherosclerosis* **203**, 1-7
6. Abifadel, M., Varret, M., Rabes, J. P., Allard, D., Ouguerram, K., Devillers, M., Cruaud, C., Benjannet, S., Wickham, L., Erlich, D., Derre, A., Villeger, L., Farnier, M., Beucler, I., Bruckert, E., Chambaz, J., Chanu, B., Lecerf, J. M., Luc, G., Moulin, P., Weissenbach, J., Prat, A., Krempf, M., Junien, C., Seidah, N. G., and Boileau, C. (2003) *Nat Genet* **34**, 154-156
7. Cohen, J., Pertsemlidis, A., Kotowski, I. K., Graham, R., Garcia, C. K., and Hobbs, H. H. (2005) *Nat Genet* **37**, 161-165
8. Cohen, J. C., Boerwinkle, E., Mosley, T. H., Jr., and Hobbs, H. H. (2006) *N Engl J Med* **354**, 1264-1272
9. Kotowski, I. K., Pertsemlidis, A., Luke, A., Cooper, R. S., Vega, G. L., Cohen, J. C., and Hobbs, H. H. (2006) *Am J Hum Genet* **78**, 410-422

10. Hooper, A. J., Marais, A. D., Tanyanyiwa, D. M., and Burnett, J. R. (2007) *Atherosclerosis* **193**, 445-448
11. Zhao, Z., Tuakli-Wosornu, Y., Lagace, T. A., Kinch, L., Grishin, N. V., Horton, J. D., Cohen, J. C., and Hobbs, H. H. (2006) *Am J Hum Genet* **79**, 514-523
12. Horton, J. D., Cohen, J. C., and Hobbs, H. H. (2009) *J Lipid Res* **50 Suppl**, S172-177
13. Piper, D. E., Jackson, S., Liu, Q., Romanow, W. G., Shetterly, S., Thibault, S. T., Shan, B., and Walker, N. P. (2007) *Structure* **15**, 545-552
14. Bottomley, M. J., Cirillo, A., Orsatti, L., Ruggeri, L., Fisher, T. S., Santoro, J. C., Cummings, R. T., Cubbon, R. M., Lo Surdo, P., Calzetta, A., Noto, A., Baysarowich, J., Mattu, M., Talamo, F., De Francesco, R., Sparrow, C. P., Sitlani, A., and Carfi, A. (2009) *J Biol Chem* **284**, 1313-1323
15. Nassoury, N., Blasiole, D. A., Tebon Oler, A., Benjannet, S., Hamelin, J., Poupon, V., McPherson, P. S., Attie, A. D., Prat, A., and Seidah, N. G. (2007) *Traffic* **8**, 718-732
16. Ni, Y. G., Condra, J. H., Orsatti, L., Shen, X., Di Marco, S., Pandit, S., Bottomley, M. J., Ruggeri, L., Cummings, R. T., Cubbon, R. M., Santoro, J. C., Ehrhardt, A., Lewis, D., Fisher, T. S., Ha, S., Njimoluh, L., Wood, D. D., Hammond, H. A., Wisniewski, D., Volpari, C., Noto, A., Lo Surdo, P., Hubbard, B., Carfi, A., and Sitlani, A. (2010) *J Biol Chem* **285**, 12882-12891
17. Zhang, D. W., Garuti, R., Tang, W. J., Cohen, J. C., and Hobbs, H. H. (2008) *Proc Natl Acad Sci U S A* **105**, 13045-13050
18. Abifadel, M., Pakradouni, J., Collin, M., Samson-Bouma, M. E., Varret, M., Rabes, J. P., and Boileau, C. (2010) *Expert Opin Ther Pat* **20**, 1547-1571
19. Chan, J. C., Piper, D. E., Cao, Q., Liu, D., King, C., Wang, W., Tang, J., Liu, Q., Higbee, J., Xia, Z., Di, Y., Shetterly, S., Arimura, Z., Salomonis, H., Romanow, W. G., Thibault, S. T., Zhang, R., Cao, P., Yang, X. P., Yu, T., Lu, M., Retter, M. W., Kwon, G., Henne, K., Pan, O., Tsai, M. M., Fuchslocher, B., Yang, E., Zhou, L., Lee, K. J., Daris, M., Sheng, J., Wang, Y., Shen, W. D., Yeh, W. C., Emery, M., Walker, N. P., Shan, B., Schwarz, M., and Jackson, S. M. (2009) *Proc Natl Acad Sci U S A* **106**, 9820-9825
20. Ni, Y. G., Di Marco, S., Condra, J. H., Peterson, L. B., Wang, W., Wang, F., Pandit, S., Hammond, H. A., Rosa, R., Cummings, R. T., Wood, D. D., Liu, X., Bottomley, M. J., Shen, X., Cubbon, R. M., Wang, S. P., Johns, D. G., Volpari, C., Hamuro, L., Chin, J., Huang, L., Zhao, J. Z., Vitelli, S., Haytko, P., Wisniewski, D., Mitnaul, L. J., Sparrow, C. P., Hubbard, B., Carfi, A., and Sitlani, A. (2011) *J Lipid Res* **52**, 78-86
21. Liang, H., Chaparro-Riggers, J., Strop, P., Geng, T., Sutton, J. E., Tsai, D., Bai, L., Abdiche, Y., Dilley, J., Yu, J., Wu, S., Chin, S. M., Lee, N. A., Rossi, A., Lin, J. C., Rajpal, A., Pons, J., and Shelton, D. L. (in print) *J Pharmacol Exp Ther*
22. Igawa, T., Ishii, S., Tachibana, T., Maeda, A., Higuchi, Y., Shimaoka, S., Moriyama, C., Watanabe, T., Takubo, R., Doi, Y., Wakabayashi, T., Hayasaka, A., Kadono, S., Miyazaki, T., Haraya, K., Sekimori, Y., Kojima, T., Nabuchi, Y., Aso, Y., Kawabe, Y., and Hattori, K. (2010) *Nat Biotechnol* **28**, 1203-1207
23. Murtaugh, M. L., Fanning, S. W., Sharma, T. M., Terry, A. M., and Horn, J. R. *Protein Sci* **20**, 1619-1631
24. Sarkar, C. A., Lowenhaupt, K., Horan, T., Boone, T. C., Tidor, B., and Lauffenburger, D. A. (2002) *Nat Biotechnol* **20**, 908-913

25. Roopenian, D. C., Christianson, G. J., Sproule, T. J., Brown, A. C., Akilesh, S., Jung, N., Petkova, S., Avanessian, L., Choi, E. Y., Shaffer, D. J., Eden, P. A., and Anderson, C. L. (2003) *J Immunol* **170**, 3528-3533
26. Tabrizi, M., Bornstein, G. G., and Suria, H. (2009) *Aaps J* **12**, 33-43
27. Dirks, N. L., and Meibohm, B. (2010) *Clin Pharmacokinet* **49**, 633-659
28. Wang, W., Wang, E. Q., and Balthasar, J. P. (2008) *Clin Pharmacol Ther* **84**, 548-558
29. Tabrizi, M. A., Tseng, C. M., and Roskos, L. K. (2006) *Drug Discov Today* **11**, 81-88
30. Rehlaender, B. N., and Cho, M. J. (1998) *Pharm Res* **15**, 1652-1656
31. Hayashi, N., Tsukamoto, Y., Sallas, W. M., and Lowe, P. J. (2007) *Br J Clin Pharmacol* **63**, 548-561
32. Maeda, K., Kato, Y., and Sugiyama, Y. (2002) *J Control Release* **82**, 71-82
33. Raghavan, M., Bonagura, V. R., Morrison, S. L., and Bjorkman, P. J. (1995) *Biochemistry* **34**, 14649-14657

FOOTNOTES

We thank S. Michael Chin, Amber Pham, Ishita Barman and Charles Appah for expressing and purifying proteins; Dan Malashock, Mayumi Pierce and Yasmina Abdiche for providing Biosensor support; Kapil Mayawala and Jake Glanville for modeling; and Wenwu Zhai for initiating the project.

The abbreviations used are: PCSK9, Proprotein Convertase Substilisin Kexin type 9; LDL, Low Density Lipoprotein; LDL-C, LDL-cholesterol; PK, pharmacokinetics; LDLR, Low Density Lipoprotein receptor; HDL, High Density Lipoprotein; FcRn, neonatal Fc receptor; CHD, coronary heart disease; CHRD, C-terminal cysteine/histidine-rich domain; EGF-A, epidermal growth factor-like repeat A; PD, pharmacodynamics; CDR, complementarity determining regions; SPR, surface plasmon resonance; i.p., intra-peritoneal; i.v., intra-venous; FcγR, Fcγ receptor; GCSF, granulocyte colony-stimulating factor; SAA, serum amyloid A; CRP, C-reactive protein.

FIGURE LEGENDS

Table 1

pH-dependent binding kinetics of J10, J16 and J17 against PCSK9 of mouse, cynomolgus and human sources at 37ºC. The standard deviations are mentioned in brackets.

Fig. 1. Serum antibody concentrations after J16 or J10 treatment. A. Total plasma J16 antibody concentration in cynomolgus monkey after a single dose of 0.1 (square), 1 (triangle), 3 (circle), 10 (inverted triangle) and 100 (diamond) mg/kg J16 over time. Results are expressed as mean ± SEM, n=4/group. **B and C:** Total serum J10 (circle) and an isotype control (square) antibody concentration in wild type (**B**) and *PCSK9* $^{-/-}$ (**C**) mice after a single dose of 10 mg/kg antibodies over time. Antibodies were dosed as a bolus i.v. injection on day 0. Results are expressed as mean ± SEM, n=8 to 9/group.

Fig. 2. PK and PD of J17 in mice and non-human primates. A and B. Serum antibody concentrations (**A**) and total cholesterol (**B**) in wild type mice dosed with a single dose of 1 (square), 3 (triangle), and 10 (circle) mg/kg of J10 (blue), J16 (red) and isotype control antibody (10 mg/kg only, black). Results are expressed as mean ± SEM, n=6 to 8/group. **C and D.** Total antibody concentrations (**C**) and the percentage of baseline (day -2) LDL-C (**D**) and in cynomolgus monkey treated with a single i.v. injection of 1.5 mg/kg of J16 (square) and J17 (triangle) on day 0. Results are expressed as mean ± SEM, n=4/group.

Fig. 3. J17, J16 and PCSK9 co-localization with LAMP2 in HepG2 cells. A. Isotype Control (IC, top row), J10 (middle row) and J17 (bottom row) antibodies are shown in red and Lamp2 in green. Images shown are maximum intensity projections from independent channels with the merged image on the middle right column. Far right column depicts co-localization mask between the two channels. Scale bar = 10 μm. **B.** Percentage of J10 and J17 puncta co-localized with Lamp2 positive puncta (left). Percentage of PCSK9 puncta co-localized with Lamp2 positive puncta in the presence of IC, J10 and J17 (right). Results are plotted as averages ± SEM of 3 independent experiments. *: p=0.0166 by students t-test.

Fig. 4. The effect of PCSK9 or FcRn knockout on J17 serum half-life. A: Antibody concentrations in *PCSK9* $^{-/-}$ mice after i.p. injection of 10mg/kg of J10 (blue circle), J17 (red square) and an isotype control antibody (black triangle) on day 0, and i.v. injection of 3mg/kg of recombinant human PCSK9 (huPCSK9) on day 15. n=3/group. **B:** Antibody concentrations in *FCRN* $^{-/-}$ mice after i.v. injection of 10mg/kg of J10 (blue circle), J17 (red square) and isotype control antibody (black triangle) on day 0. n=7/group. Results are expressed as mean ± SEM.

Table 1
Binding kinetics of J10, J16 and J17 against mouse, cyno and humanPCSK9 at pH6.0 and pH7.4. Experiments were done at 37ºC. The standard deviations of replicate experiments are shown in brackets. All experiments were run in triplicate, except for the J10/hPCSK9 interaction at pH 6.0 which was run in duplicate.

		pH 6.0			**pH 7.4**			**Ratios**	
Antibody	Antigen	k_a (x 10^5 M^{-1} s^{-1})	k_d (x 10^{-3} s^{-1})	K_D (nM)	k_a (x 10^5 M^{-1} s^{-1})	k_d (x 10^{-3} s^{-1})	K_D (nM)	$K_{D,\ pH\ 6}$ / $K_{D,\ pH\ 7.4}$	$k_{d,\ pH\ 6}$ / $k_{d,\ pH\ 7.4}$
J10	mPCSK9	8.2 (0.2)	1.8 (0.01)	2.2 (0.05)	6.5 (0.2)	1.3 (0.02)	2.0 (0.03)	0.9	1.4
J16	mPCSK9	9.0(0.2)	0.43 (0.002)	0.47(0.01)	10 (1)	0.29 (0.002)	0.28 (0.02)	1.7	1.5
J17	mPCSK9	6.9 (1.4)	7.7 (0.8)	11 (1)	7.8 (0.8)	2.3 (0.2)	2.9 (0.5)	3.8	3.3
J10	cyPCSK9	8.1 (0.2)	0.54 (0.01)	0.66 (0.01)	7.5 (0.5)	0.40 (0.02)	0.54 (0.04)	1.2	1.4
J16	cyPCSK9	9.5(1.4)	0.16(0.002)	0.17(0.02)	11 (4)	0.12 (0.01)	0.12 (0.04)	1.4	1.3
J17	cyPCSK9	33 (3)	12 (1)	3.7 (0.2)	7.4 (0.2)	1.0 (0.04)	1.4 (0.02)	2.6	12
J10	hPCSK9	8.3 (0.3)	0.48 (0.005)	0.58 (0.02)	10 (0.2)	0.34 (0.01)	0.34 (0.01)	1.7	1.4
J16	hPCSK9	14 (0.07)	0.19(0.004)	0.13(0.003)	15 (0.2)	0.15 (0.004)	0.10 (0.002)	1.3	1.3
J17	hPCSK9	13 (1)	4.6(0.1)	3.5(0.2)	16 (0.3)	0.60 (0.004)	0.38 (0.01)	9.2	7.7

Fig. 1

A

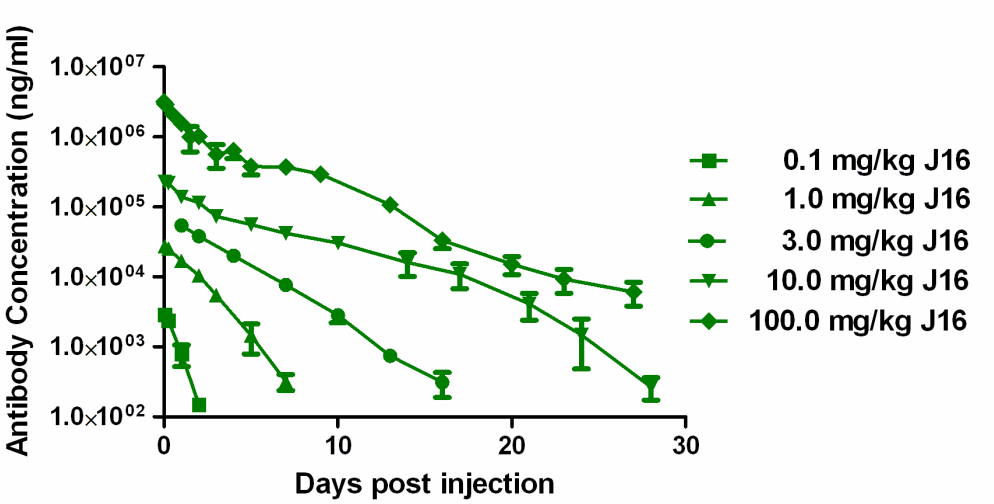

B

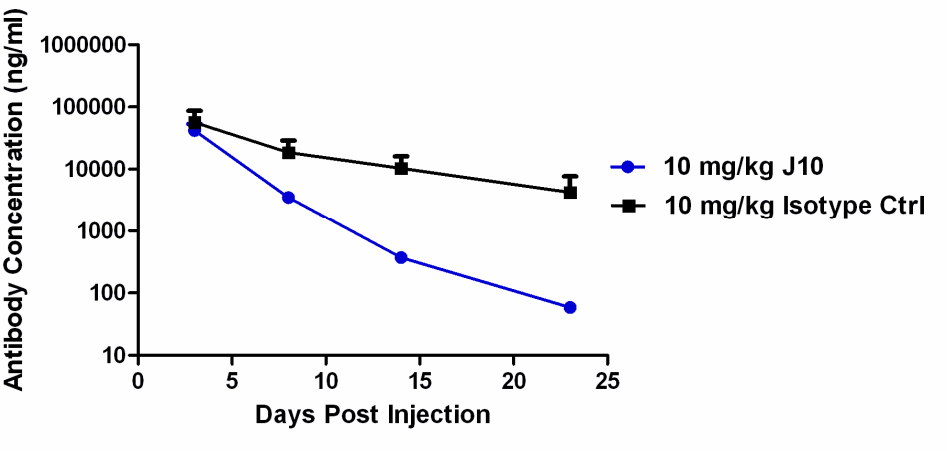

C

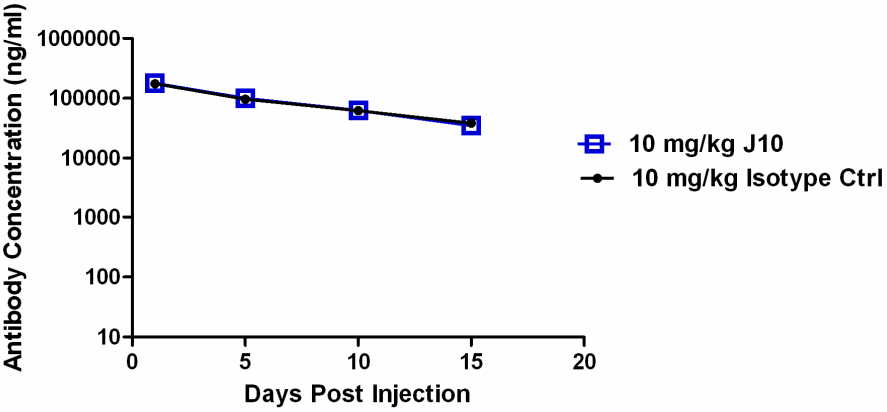

Fig. 2

A

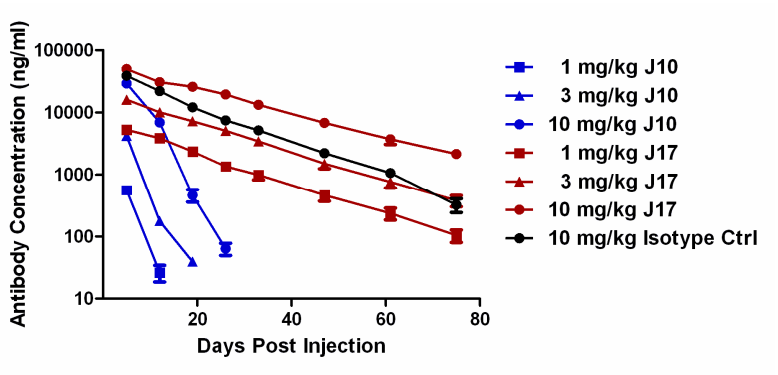

B

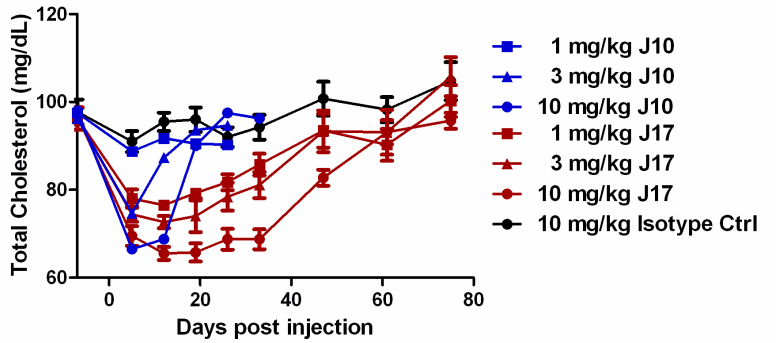

C

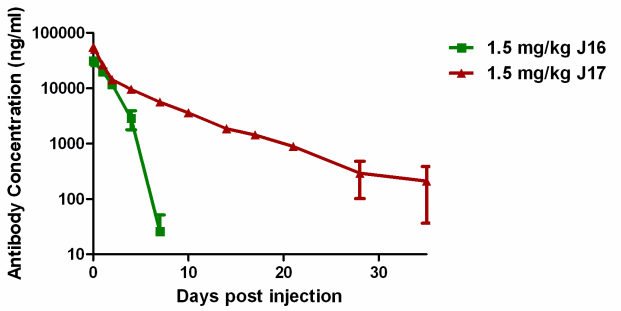

D

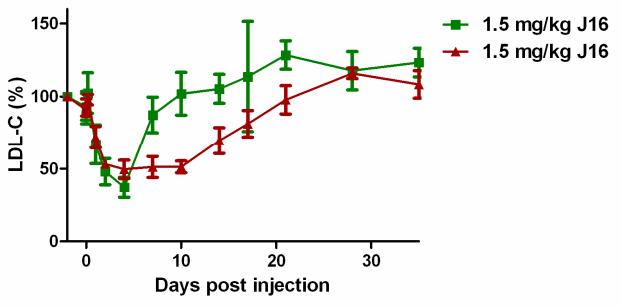

Fig. 3

A

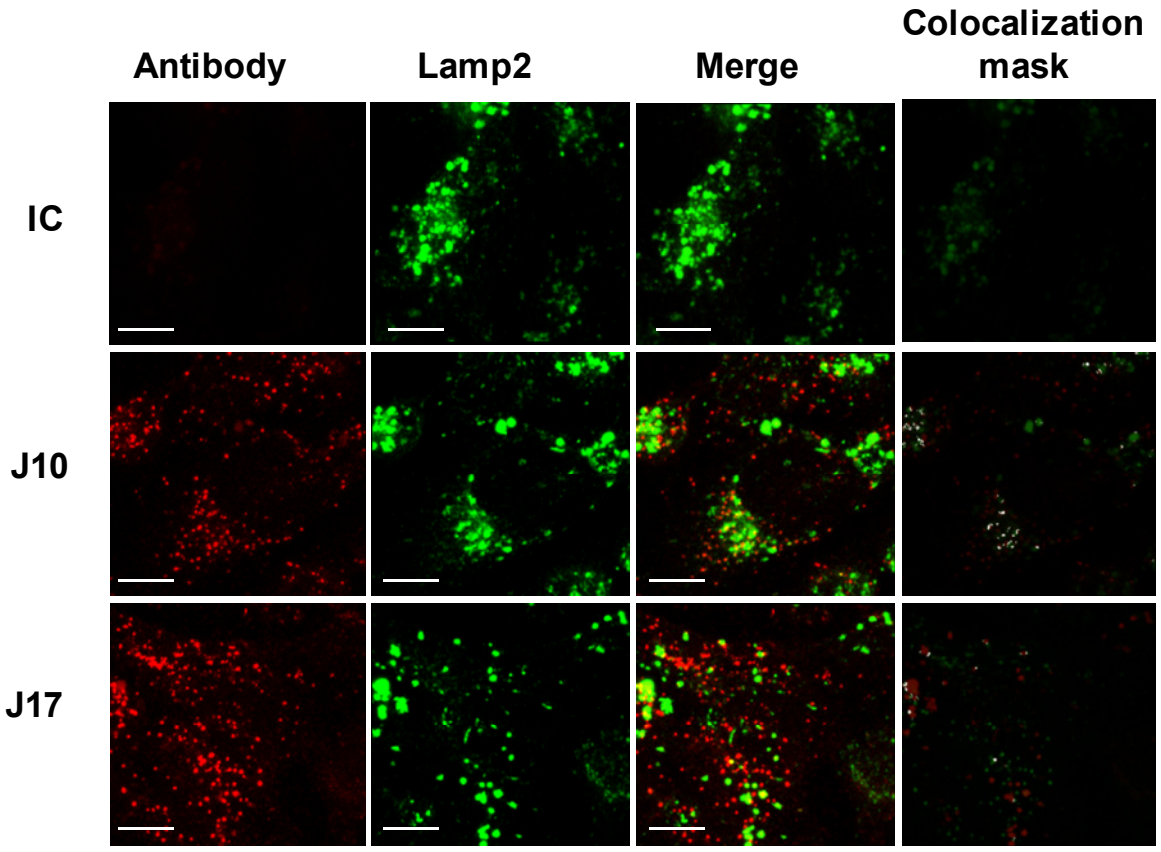

B

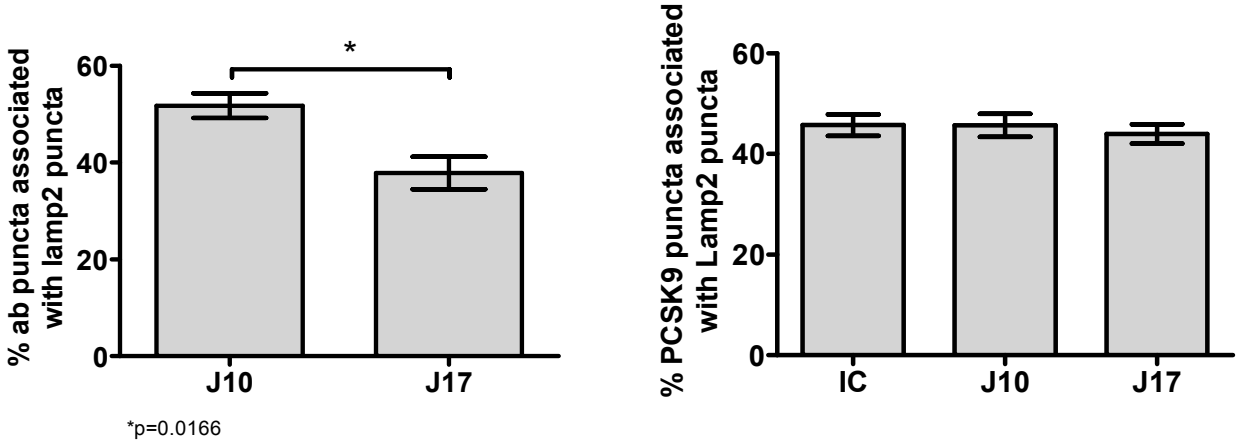

Fig. 4

A

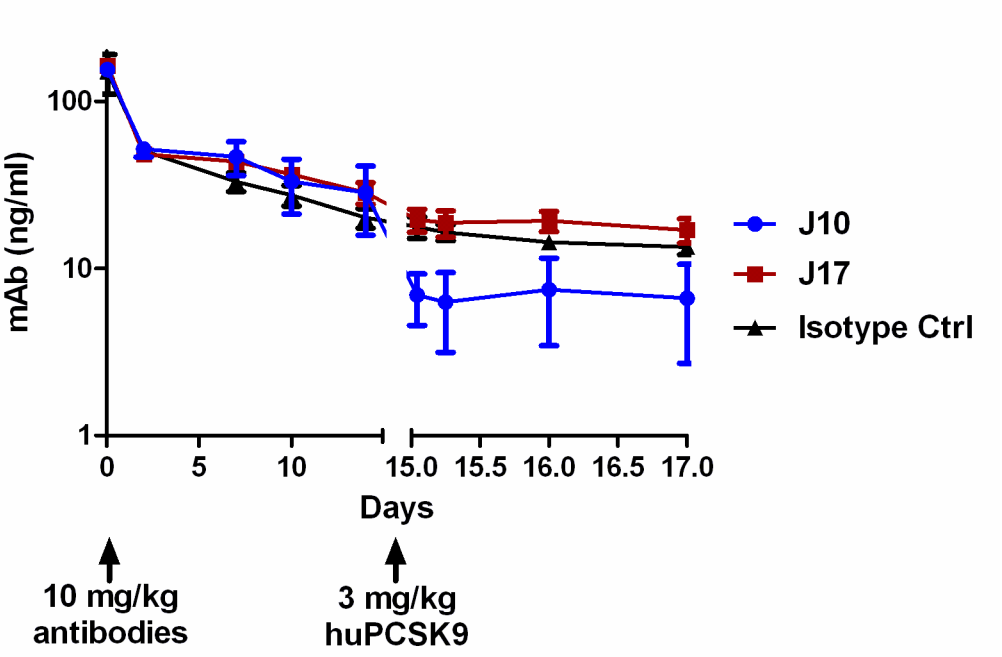

B